



# Epstein–Barr Virus+ B Cells in Breast Cancer Immune Response: A Case Report

Andrea Aran<sup>1</sup>, Vicente Peg<sup>2</sup>, Rosa Maria Rabanal<sup>3</sup>, Cristina Bernadó<sup>4</sup>, Esther Zamora<sup>5</sup>, Elisa Molina<sup>1</sup>, Yago A. Arribas<sup>1</sup>, Joaquín Arribas<sup>4,6,7,8</sup>, José Pérez<sup>9</sup>, Carme Roura-Mir<sup>1</sup>, Montserrat Carrascal<sup>10</sup>, Javier Cortés<sup>5,9</sup> and Mercè Martí<sup>1\*</sup>

<sup>1</sup> Immunology Unit, Department of Cell Biology, Physiology and Immunology, Institut de Biotecnologia i Biomedicina (IBB), Universitat Autònoma de Barcelona (UAB), Bellaterra, Spain, <sup>2</sup> Translational Molecular Pathology, Vall d'Hebron Institut de Recerca (VHIR), Barcelona, Spain, <sup>3</sup> Unitat de Patologia Murina i Comparada, Department of Animal Medicine and Surgery, Veterinary Faculty, Universitat Autònoma de Barcelona (UAB), Barcelona, Spain, <sup>4</sup> Preclinical and Translational Research Program, Vall d'Hebron Institute of Oncology (VHIO), Barcelona, Spain, <sup>5</sup> Breast Cancer Unit, Vall d'Hebron Institute of Oncology (VHIO), Hospital Universitari Vall d'Hebron, Barcelona, Spain, <sup>6</sup> Cancer Research Program, Hospital del Mar Medical Research Institute (IMIM), Barcelona, Spain, <sup>7</sup> Centro de Investigación Biomédica en Red de Cáncer, Madrid, Spain, <sup>8</sup> Institució Catalana de Recerca i Estudis Avançats (ICREA), Barcelona, Spain, <sup>9</sup> International Breast Cancer Center (BCC), Quironsalud Group, Barcelona, Spain, <sup>10</sup> Biological and Environmental Proteomics, Institute of Biomedical Research of Barcelona, Spanish National Research Council, Institut d'Investigacions Biomèdiques August Pi i Sunyer (IIBB-CSIC/IDIBAPS), Barcelona, Spain

## OPEN ACCESS

### Edited by:

Zong Sheng Guo,  
Roswell Park Comprehensive Cancer  
Center, United States

### Reviewed by:

Bingliang Fang,  
University of Texas MD Anderson  
Cancer Center, United States  
Frank Momburg,  
German Cancer Research Center  
(DKFZ), Germany

### \*Correspondence:

Mercè Martí  
merce.marti@uab.cat

### Specialty section:

This article was submitted to  
Cancer Immunity  
and Immunotherapy,  
a section of the journal  
Frontiers in Immunology

**Received:** 20 August 2021

**Accepted:** 21 October 2021

**Published:** 16 November 2021

### Citation:

Aran A, Peg V, Rabanal RM, Bernadó C, Zamora E, Molina E, Arribas YA, Arribas J, Pérez J, Roura-Mir C, Carrascal M, Cortés J and Martí M (2021) Epstein–Barr Virus+ B Cells in Breast Cancer Immune Response: A Case Report. *Front. Immunol.* 12:761798. doi: 10.3389/fimmu.2021.761798

EBV-specific T cells have been recently described to be involved in fatal encephalitis and myocarditis in cancer patients after immune checkpoint therapies. Here, we report the study of a human triple-negative breast cancer tumor (TNBC) and EBV-transformed B cells obtained from a patient-derived xenograft (PDX) that progressed into a lymphocytic neoplasm named xenograft-associated B-cell lymphoma (XABCL). T-cell receptor (TCR) high-throughput sequencing was performed to monitor the T-cell clonotypes present in the different samples. Forty-three T-cell clonotypes were found infiltrating the XABCL tissue after three passes in mice along 6 months. Eighteen of these (42%) were also found in the TNBC biopsy. TCR infiltrating the XABCL tissue showed a very restricted T-cell repertoire as compared with the biopsy-infiltrating T cells. Consequently, T cells derived from the TNBC biopsy were expanded in the presence of the B-cell line obtained from the XABCL (XABCL-LCL), after which the TCR repertoire obtained was again very restricted, i.e., only certain clonotypes were selected by the B cells. A number of these TCRs had previously been reported as sequences involved in infection, cancer, and/or autoimmunity. We then analyzed the immunopeptidome from the XABCL-LCL, to identify putative B-cell-associated peptides that might have been expanding these T cells. The HLA class I and class II-associated peptides from XABCL-LCL were then compared with published repertoires from LCL of different HLA typing. Proteins from the antigen processing and presentation pathway remained significantly enriched in the XABCL-LCL repertoire. Interestingly, some class II-presented peptides were derived from cancer-related proteins. These results suggest that bystander tumor-infiltrating EBV+ B cells acting as APC may be able to interact with tumor-infiltrating T cells and influence the TCR repertoire in the tumor site.

**Keywords:** Epstein–Barr virus, B cells, T cells, breast cancer, TCR—T-cell receptor

## 1 INTRODUCTION

The immune system plays a key role in cancer, but differences between individuals can lead to different outcomes. A high number of tumor-infiltrating lymphocytes (TIL) in triple-negative breast cancer (TNBC) are related to a better prognosis (1), although not in all patients (2). Several factors influence a good antitumoral immune response, such as the recognition of neoantigens, the presence of immunomodulatory mediators, or the cellular composition and diversity of TIL, including the presence of antigen-presenting cells (APC) such as dendritic cells (DC) or B cells. DC can migrate from the tumor site to the proximal lymph nodes to activate antigen-specific T cells, but the presence of APC in the tumor site is also necessary for the maintenance of cytotoxic T lymphocytes (CTL) and T helper (Th) cells. In the last years, tumor-associated B cells have been gaining interest and their presence has been associated with a good prognosis in breast cancer (3), colorectal cancer (4), ovarian cancer (5), hepatocellular carcinoma (6), soft sarcoma (7), and lung cancer (8), among others. Nevertheless, the role of B cells as active APC in the tumor site is not well established.

B cells are also the main targets of the Epstein–Barr virus (EBV) (9). Asymptomatic infections of young children by EBV are very common, so it is not surprising that EBV-infected cells (EBV+ B cells) are found among TIL (10) in many cancer types. EBV was the first recognized human oncovirus when it was isolated from a Burkitt lymphoma patient (9). Nowadays, the relationship between EBV infection and several lymphomas, i.e., Burkitt lymphoma (9, 11), Hodgkin's lymphoma (12, 13), and posttransplant lymphoproliferative disorder (14, 15) is well established.

In the last years, the influence of endogenous virus in the outcome of carcinomas has been gaining evidence (16). Nevertheless, most of the studies are focused on the role of these viruses in the malignant transformation of epithelial cells, but the influence of virus-infected immune cells in the antitumoral response should also be considered. Even though epithelial cells can also be infected, B cells are the natural reservoir of EBV (17). Moreover, immunomodulatory effects are more likely to occur when the EBV infects B cells rather than epithelial cells since some tumor epithelial cells can downregulate the expression of HLA class I molecules (18).

EBV can be maintained for life in hosts because it has the capacity to persist in a latent state. It is well known that EBV can take advantage of the immunosuppression status of individuals (19) as suggested by the increase of lymphoma incidence in HIV-infected and organ-transplanted patients (20). This was supported by Mazar's group who reported that 32% of patient-derived xenograft (PDX) tumors generated from epithelial tumor material can progress into EBV+ lymphocytic neoplasms (10)—or xenograft-associated B-cell lymphoma (XABCL) reported in other studies (21, 22)—evidencing the presence of EBV+ cells within the tumor material. The NOD SCID gamma (NSG) mice, used for PDX generation, are likely more susceptible to EBV-associated malignancies due to the lack of T-cell immune responses. Our proposal is that the presence of EBV+ B cells within a tumor may shape the antitumoral immune response.

EBV+ B cells in an infectious stage of the virus induce a strong T-cell-specific response (23). However, under the influence of the tumor microenvironment and/or of immunomodulatory treatments, the behavior, response, and repertoire of tumor-infiltrating cells—not only tumor-specific T cells but also bystander EBV-specific T cells—can be affected. This would give an opportunity for EBV in an infectious stage to survive but also could have long-term consequences affecting the immune system. The presence of EBV-specific T cells among tumor infiltrates has been described, and in two recent studies, their involvement in fatal inflammatory processes was suggested [myocarditis (24) and encephalitis (25)] in melanoma patients after immune checkpoint inhibitor (ICPI) therapies.

The aim of this study was to determine the relationship between tumor-infiltrating T and EBV+ B cells from a TNBC patient. To our knowledge, this is the first time that B cells generated in a XABCL have been used as an autologous EBV lymphoblastoid cell line (LCL) to study these B-cell–TIL interactions. T-cell receptor (TCR) and B-cell receptor (BCR) analyses were performed to study the presence of tumoral-infiltrating lymphocytes in the TNBC tumor as well as to monitor T-cell expansions. Our data as a first proof of concept have demonstrated that TIL derived from the breast cancer infiltrate can be maintained for at least 6 months in the XABCL, but also that certain clonotypes can be expanded *in vitro* in the presence of the established B-cell line derived from the XABCL (XABCL-LCL). Some of the TCRs involved have been previously described in cancer, but also in infections and autoimmunity. The whole peptide repertoire presented by HLA-ABC and HLA-DR from XABCL-LCL was also investigated and compared with LCL peptidomes from the literature. The characterization of the specific proteins from which these peptides were derived indicated that most of them were related with antigen processing and presentation pathways, suggesting that the XABCL-LCL can act as a strong APC. We have also assessed whether some of the proteins identified in the immunopeptidome had a relationship with cancer, and interestingly, most of the cancer-associated proteins were presented by class II molecules. In summary, this study suggests that EBV+ bystander B cells present in the tumor can interact with tumor-infiltrating T cells by acting as APC, thus participating in the antitumor response and influencing the outcome of the patient.

## 2 MATERIAL AND METHODS

### 2.1 Samples and Cell Cultures

#### 2.1.1 TNBC Biopsy

The biopsy Breast Cancer-Patient Sample-562 (BC-PS-562) was obtained from surplus hospital material, donated by the Vall d'Hebron Institute of Oncology (VHIO), by standard procedures with the appropriate approval of the Ethical and Scientific Committee of the institution. Consent was obtained from the patient according to local institutional review board requirement. The TNBC core biopsy was cut in several slices: five slices were

frozen in liquid nitrogen and seven slices were cultured on a 48-well plate. Biopsy-derived T-cell clones were cultured in 1 ml of Iscove's modified Dulbecco's medium (IMDM) GlutaMAX™ (Gibco) supplemented with 1% penicillin–streptomycin, 10% of decompartmented human serum, and IL-2 (100 U/ml) (provided by the NIH). For this study, only the three tissue frozen slices were used as a source of the original tumoral tissue, and the cultures derived from four of the slices were used to study the T cells in culture derived from the explants.

### 2.1.2 XABCL Generation

PDX mice (PDX-562) were generated by implanting a TNBC (BC-PS-562) core biopsy into NOD SCID mice. After three passes, the tumoral tissue was obtained. The tumor was collected in PBS and disaggregated by using a scalpel. Crushed tissue was resuspended in 5 ml of DMEM/F12 (Gibco) complemented with 10% of fetal bovine serum (Gibco), 1% L-glutamine (Biowest), 1% penicillin–streptomycin (Sigma-Aldrich), and 300 U/ml of collagenase type IA (Sigma-Aldrich) and incubated twice in a shaker 80×g and 37°C during 30 min. After centrifuging the disaggregated tissue, 100- and 40-µm pore cell strainers were used to obtain a uniform single-cell suspension from the cell pellet.

### 2.1.3 XABCL-LCL Culture

After tissue digestion of the XABCL tumoral tissue, B cells were cultured and grown to a final concentration of  $3 \times 10^5$  cells/ml in T75 flasks using RPMI GlutaMAX™ (Gibco) with 1% penicillin and streptomycin (Sigma-Aldrich) and 10% of Fetal Bovine Serum (Gibco).

### 2.1.4 TNBC-T Cells and XABCL-LCL Co-Cultures

To select XABCL-reactive T cells, TNBC-T cells from one of the tissue slices were grown for 10 days in culture medium without cell-specific stimulus. Cells were grown at a final concentration of  $3 \times 10^5$  cells/ml with IMDM GlutaMAX™ (Gibco) complemented with 10% of human serum, 1% penicillin–streptomycin (Sigma-Aldrich), and IL-2 at 100 U/ml in contact with XABCL-LCL B cells and allogeneic PBMCs, previously irradiated at 60 and 30 Gy, respectively. On the 7–10th day, cells were restimulated using anti-human CD3 and anti-CD28-coated Dynabeads (Gibco). As a control, cells were grown using a rapid expansion method (REM) (26). T cells ( $1–1.5 \times 10^5$ ) were cultured in the presence of feeders ( $25 \times 10^6$  30 Gy irradiated PBMCs) in a T25 flask with 25 ml of complete medium (IMDM GlutaMAX™ with 1% P/S and 10% of decompartmented human serum) supplemented with 50 ng/ml of soluble anti-CD3 (OKT3) and IL-2 at 200 U/ml. On the fifth day, half of the medium was removed and replaced with fresh medium with IL-2 at 200 U/ml, and cells were collected 10–12 days after stimulation.

## 2.2 Tumoral and T- and B-Cell Presence in the Biopsy

### 2.2.1 Immunohistochemistry

The presence of tumoral cells and infiltrating T and B cells in the biopsies was determined by hematoxylin and eosin (HE) and

immunohistochemistry (IHC). Antibodies used for the paraffin-embedded sections of the TNBC biopsy were anti-human CD3 (clone 2GV6), anti-human CD4 (clone SP35), anti-human CD8 (clone SP57), and anti-human CD20 (clone L26) (Ventana Medical System, Inc.). IHC of the XABCL tissue was performed in samples fixed in 10% neutral buffered formalin. Transverse sections were used for processing. Morphological evaluation was performed on 5-µm paraffin-embedded sections, stained with HE. The primary antibodies used were rabbit polyclonal anti-human CD3 (Dako) and rabbit polyclonal anti-human CD20 (Thermo Fisher). Sections were incubated with a labeled polymer [anti-rabbit for CD3 and CD20 (Agilent-Dako)] according to the instructions of the manufacturer. IHC was completed using 3,3'-diaminobenzidine (DAB) and counterstaining in hematoxylin. Positive controls of the XABCL IHC were performed using normal mouse spleen and lymph node. In all the experiments, for the negative control, an isotype-specific immunoglobulin was used to substitute the primary antibody as negative control; no immunostaining was detected in these sections.

## 2.3 Characterization of XABCL-LCL and TNBC-T Cells

### 2.3.1 Phenotypic Characterization of T and B Cells

Between  $2$  and  $5 \times 10^5$  of cells were stained with anti-human antibodies for 20 min at 4°C in the dark with PBS containing 2% FBS. After incubation, cells were washed twice, collected in 200 µl of PBS, and analyzed by flow cytometry.

For the XABCL-LCL phenotype analysis, anti-human antibodies used were PE-conjugated anti-CD19 (BD Pharmingen), PE-conjugated anti-CD20, FITC-conjugated anti-CD21, PE-Cy7-conjugated anti-CD38, APC-conjugated anti-HLA-ABC (BD Pharmingen), PE-conjugated anti-HLA-DR (BD Pharmingen), FITC-conjugated anti-CD80 (ImmunoTools), FITC-conjugated anti-CD86 (ImmunoTools), PE-conjugated anti-PD-1 (eBioscience), and FITC-conjugated anti-PD-L1 (BD Pharmingen). For the T-cell phenotype analysis, the following human antibodies were used: PerCP-conjugated anti-human CD3, PE-conjugated anti-human or FITC-conjugated anti-human CD4, and FITC-conjugated anti-human CD8 or APC-conjugated anti-human CD8 (BD Pharmingen). The flow cytometer used was BD FACS Canto. Analyses were performed by using the FlowJo and FACS Diva software.

### 2.3.2 BCR and TCR High-Throughput Sequencing of TNBC, XABCL, TNBC-T Cells, and XABCL-LCL

DNA extraction from the TNBC and XABCL tissues and XABCL-LCL was carried out using a phenol–chloroform protocol. Tissue samples were disrupted by sonication. Amplification of BCR and TCR transcripts from DNA was performed using survey level ImmunoSEQ technology by Adaptive Biotechnologies. For the high-throughput sequencing (HTS) of TNBC-T cells, cells were counted and between  $1 \times 10^5$  and  $1 \times 10^6$  of T cells from the initial cultures and expanded T cells were used for RNA extraction. RNA was isolated using

RNeasy Micro Kit and RNeasy Mini Kit (Qiagen), respectively, following the instructions of the manufacturer. An optional on-column DNase digestion was also performed during the RNA isolation using the RNase-Free DNase Set (Qiagen). RNA amounts and integrity were measured with Agilent 2100 bioanalyzer (Agilent Technologies). Human TCR profiling from TIL was assessed by using the SMARTer Human TCR a/b Profiling Kit (Takara Bio), which allows the complete capture of V(D)J variable regions of TCR transcripts and library production, directly indexed for sequencing. Both TCR-alpha and TCR-beta chain diversities were studied. Purification of amplified libraries was performed using Agencourt AMPure XP Beads (Beckman Coulter), following the commercial recommendations. Analysis and validations of libraries were carried out on an Agilent 2100 Bioanalyzer, using the DNA 1000 Kit (Agilent Technologies). Sequence was performed on an Illumina MiSeq sequencer using the 600-cycle MiSeq Reagent Kit v3 (Illumina) with paired-end 2 × 300 base pair reads.

### 2.3.3 TCR and BCR Repertoire Analysis

TCR and BCR sequencing results obtained from the ImmunoSEQ analysis were evaluated by the ImmunoSEQ analyzer, v.3.0. TCR sequencing data obtained from the SMARTer Human TCR a/b Profiling Kit were evaluated by the MiXCR Immune Repertoire Analyzer (27). Raw data obtained from both technologies were processed using VDJTools (28). Non-productive clonotypes were excluded. The remaining repertoire data were collapsed by CDR3 amino acid sequences, i.e., clonotypes with different nucleotide sequences encoding the same CDR3 amino acid sequence were summed, and frequencies were recalculated. The different TCR and BCR sequencing results from each sample were compared to find out the common sequences shared by the XABCL, TNBC, and TNBC-T cells. Diversity and heat plot analyses were also performed using VDJTools (28). The TCR sequences obtained from this analysis were compared with the McPAS-TCR (29) database with a Levenshtein distance of 1. Figures were performed using the Graphpad Prism 7.0 software. UpSet plots were generated using R (version 3.6.1) (30) using the “dplyr,” (31) “RColorBrewer,” (32) and “UpSetR” (33) packages.

## 2.4 Characterization of the HLA-Associated Peptide Repertoire From the XABCL-LCL

### 2.4.1 Purification of Peptide–HLA Complexes

Two  $40 \times 10^6$  pellets of XABCL-LCL were used to elute peptides presented by HLA-ABC and HLA-DR. The cellular lysis was performed as described by Heyder et al. (34) Briefly, the cell pellet was resuspended in lysis buffer [50 mM Tris–HCl (pH 8.0), 150 mM NaCl, 1× Complete protease inhibitor (Roche), and 5 mM EDTA]. Nuclei and cell debris were cleared by 2× 12 min centrifugations at  $5,500 \times g$  after sonication (40% of amplitude of max. 130 W) and 10 min incubation at 4°C. Membranes collected from the supernatant were pelleted with 1 h ultracentrifugation at  $72,000 \times g$  and 4°C and resuspended in a solubilization buffer [1% n-dodecyl- $\beta$ -D-maltoside, 50 mM Tris–

HCl (pH 8.0), 150 mM NaCl, 1× Complete protease inhibitor (Roche), and 5 mM EDTA]. Solubilized pelleted membranes were sonicated 4× 5 s (20% amplitude of max. 130 W) and incubated overnight at 4°C. Non-solubilized membranes were pelleted by ultracentrifugation at  $55,000 \times g$  for 1 h at 4°C, and HLA complexes in the supernatant were then purified from the soluble fraction based on the Spetnik et al. protocol (35). Solubilized membranes were incubated overnight with 100  $\mu$ l CNBr-activated sepharose beads (GE Healthcare Life Sciences) coupled to anti-HLA-ABC w6/32 or to the anti-HLA-DR B8.11.2 antibodies. Antibody-conjugated sepharose beads were washed 3× with 50 mM Tris–HCl (pH 8.0), 150 mM NaCl, and 0.5% n-dodecyl- $\beta$ -D-maltoside and 3× with 50 mM Tris–HCl (pH 8.0) and 150 mM NaCl. Unspecific interactions were diminished by washing with a high-salt concentration buffer [50 mM Tris–HCl (pH 8.0), 0.5 M NaCl]. Peptide–HLA–DR complexes were eluted with 0.25% TFA after washing 3× with 50 mM Tris–HCl (pH 8.0) and 150 mM NaCl and 1× with 20 mM Tris–HCl (pH 8.0). The eluted complexes were cleared by SCX and a C18 tip before mass spectrometry.

### 2.4.2 Peptide Identification by Mass Spectrometry

Samples were analyzed by liquid chromatography coupled to high-resolution mass spectrometry (LC–HRMS). The LTQ Orbitrap XL mass spectrometer (Thermo Fisher) equipped with a nanoESI source and coupled to an Agilent 1100 nanochromatographic system was used. LC separation was performed using a 140-min acetonitrile gradient. Analyses were performed in data-dependent mode at a target mass resolution of 60,000 (at  $m/z$  400). Up to 10 of the most intense peaks with charge  $\geq 2$  and intensity above the 500-unit threshold were selected and fragmented by CID. To minimize the redundant selection of precursor ions, dynamic exclusion was set to 1 for 45 s. Raw data were processed using Proteome Discoverer 1.4 against the human and viral proteome database (UniProt/SwissProt) with the following parameters: no enzyme, 20 ppm precursor mass tolerance, 0.02 Da fragment tolerance, and variable modification of oxidized methionine (+16 Da). Peptide spectral matches were filtered at 1% FDR using Percolator.

### 2.4.3 HLA-Derived Peptide Repertoire Analysis

Peptides identified were prefiltered by following these rules: elimination of I) peptides outside the range 8–13mer and peptides shorter than 10-mer peptides, for class I and class II analyses, respectively; II) keratin-derived peptides; and III) duplicate peptides with modifications. The subcellular location of the source proteins was extracted from the UniProt (36) database. Proteins that were found in more than one subcellular location were counted in both localizations. DAVID (37, 38), which executes a functional annotation clustering using different databases, was used for the KEGG Pathway Database pathway enrichment analysis. For the Gibbs clustering, peptides found in nested sets were excluded, leaving only the shortest peptide.

#### 2.4.4 Identification of Proteins in the XABCL-LCL HLA Peptide Repertoire

To exclude peptides from proteins commonly presented by LCL, the source proteins of the peptides obtained in the HLA-ABC analysis were compared with 26,305 source proteins, from 6 different studies and 7, 11, and 9 different HLA-A, B, and C alleles, respectively (39–44). For the HLA-DR peptides, 517 source proteins from 10 different studies and 11 different HLA-DR alleles found in the literature (45–54) were used. The assignment of the peptides to the corresponding allele was performed according to the following criterion. First, only peptides clustered by Gibbs Cluster 2.0 (55) were used. Then, peptides predicted as strong binders by the NetMHCIPan 4.1 Server and the NetMHCIIpan 4.0 Server (56) were considered. Peptides with a peptide spectral match (PSM) of 1 were excluded. The source proteins from the peptides obtained were examined in the Human Protein Atlas (57–59) to check for specificities in cancer. The number of proteins, peptides, and PSM was considered. All data were represented using the GraphPad Prism 7.0 software.

### 3 RESULTS

#### 3.1 The Tumor Generated in a PDX Derived From the Tumor of a TNBC Patient Was the Result of a Monoclonal Expansion of EBV+ Tumor-Infiltrating B Cells

A 44-year-old patient was diagnosed with TNBC. The presence of an infiltrating ductal carcinoma [histological grade 3, no vascular invasion, estrogen receptor (ER)-negative, progesterone receptor (PR)-negative, human epidermal growth factor 2 (HER2)-negative, and Ki67 70%] was confirmed by the Pathological Anatomy Unit of the Vall d'Hebron Institute of Oncology (Barcelona, Spain).

Two core biopsies were obtained at the same time, i.e., 2 weeks after diagnosis and before neoadjuvant chemotherapy; one was inoculated in an NSG mouse to obtain a PDX and the other one was used to study the T-cell infiltration directly from the tissue or from the T-cell cultures (TNBC samples, from now on TNBC and TNBC-T cells, respectively). The TNBC (Figure 1A) was infiltrated with CD20+ B cells and CD3+ T cells (Figures 1B, C). A similar distribution was observed for both B and CD4+ T cells, suggesting that these cells could be interacting in the tumor site. Although there was a higher presence of CD4+ T cells (Figure 1D), CD8+ T cells were also found (Figure 1E).

The tumor grown in the PDX mouse was obtained after three passes in mice. Cells from this culture did not show epithelial tumor cell line characteristics, but an LCL-like phenotype. A stable long-term cell line was established from the digested tumoral tissue (XABCL-LCL, from now on). The lymphocytic origin was confirmed by IHC (Figure 2), and not only most of the cells were CD20+, but also some of these cells presented a bilobed nucleus, reminding of the Reed–Sternberg

cells associated with Hodgkin's lymphoma (12). An HLA genotyping confirmed the patient cells as the origin of the XABCL tumor (HLA-A\*02:01, A\*30:02, B\*18:01, B\*49:01, Cw\*05:01, Cw\*12:03, DRB1\*03:01, DRB1\*11:01, DQB1\*02:01, DQB1\*03:01), and we confirmed that both the XABCL-LCL and the PBMCs from the patient—but not the TNBC-T cells—were EBV+ by qPCR (data not shown). The phenotypic analysis of the XABCL-LCL revealed a molecular pattern that resembled an activated germinal center B cell, i.e., CD19+, CD20+, CD21–, and CD38+, and they also expressed HLA-ABC and HLA-DR molecules as well as CD80, CD86, and PD-L1 (Supplementary Figure 1), confirming that these cells have antigen-presenting capacities, as it was expected in a B-cell line. We could not detect antibodies in the supernatant from the XABCL-LCL culture (data not shown).

A BCR HTS revealed that one single BCR sequence, i.e., CAKDVTDVSAAYYYQAEYFPHW (IGHV03-23), represented more than the 97% of the repertoire in both samples, i.e., the XABCL tissue and the XABCL-LCL (Supplementary Table 1), confirming a monoclonal expansion produced before the *in vitro* cell line establishment. We performed the BCR HTS on the TNBC tissue and the same BCR sequence was found, confirming that the B cells that composed the XABCL were originally present within the tumor infiltrate of the patient and transformed into a monoclonal lymphocytic tumor in the mouse.

#### 3.2 XABCL B Cells Can Maintain Tumor-Infiltrating T Cells *In Vivo* and *In Vitro*

Tissue sections were obtained from each pass in mice and the IHC of the XABCL tissue revealed some CD3+ T cells infiltrating the tumor after the first pass (Supplementary Figure 2). A TCR CDR3 HTS was performed to study which infiltrating T-cell clonotypes could have remained in the XABCL tissue, obtained from mice after the third pass. The analysis revealed 43 different T-cell clonotypes where the most prevalent clone represented 31.8% of the sample (Supplementary Table 2).

To prove that the clonotypes found in the XABCL tissue came from the human biopsy, a TCR CDR3 HTS was also realized on the TNBC samples. As expected, many more clonotypes were identified: 26,724 from the TNBC and 5,451 in the TNBC-T cells. A total of 1,144 clonotypes were shared between these two sets (Figure 3A and Supplementary Table 2). Eighteen TCR sequences appeared in common between the TNBC samples and the XABCL tissue: 4 were shared by three samples, 13 were shared by TNBC and XABCL tissues, and only 1 sequence was exclusively found in the TNBC-T cells and the XABCL tissue. Only one of the four TNBC-T cell samples (slices in culture) analyzed (see *Material and Methods*) shared a TCR sequence with the XABCL.

A tracking heat plot of the 50 most abundant clonotypes—using samples with shared sequences—revealed a different pattern of TCR in the three sets, especially in the XABCL tissue (Figure 3B), i.e., the most abundant clonotypes infiltrating the XABCL after 6 months were not the most abundant in the TNBC tissue or in the TNBC-T cell sample. Thus, the XABCL model demonstrated that B cells can maintain

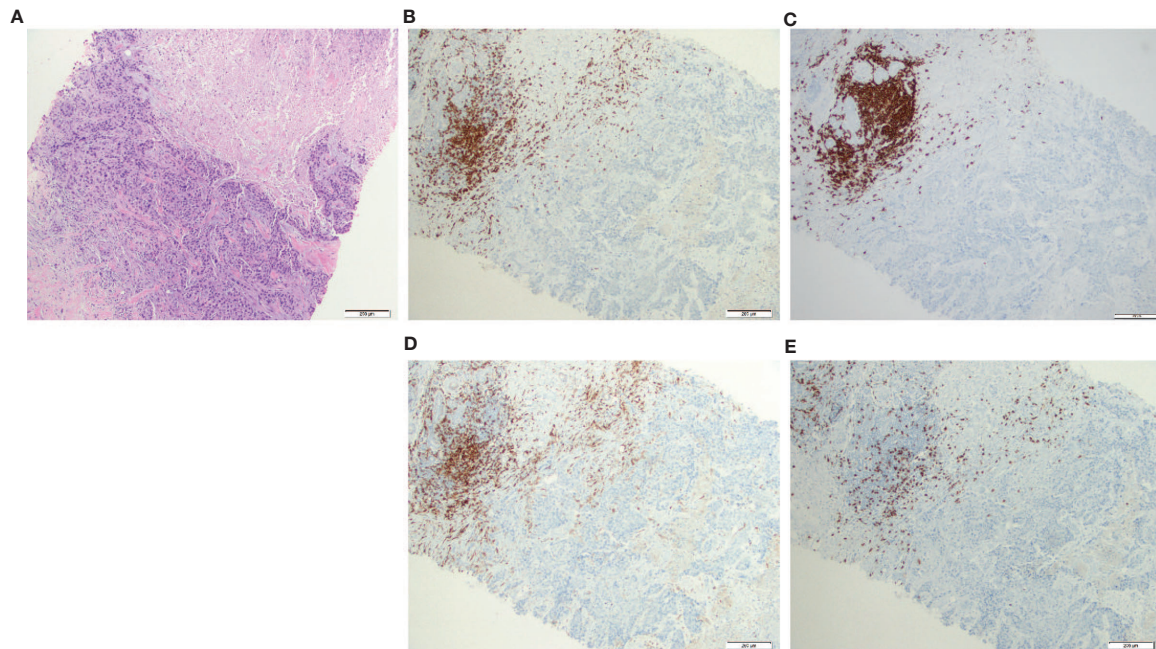


**FIGURE 1** | CD3+ T cells (both CD4+ and CD8+) and CD20+ B cells were present and colocalized in the patient biopsy. Hematoxylin and eosin (HE) staining and immunohistochemistry (IHC) from the triple-negative breast cancer (TNBC) core biopsy realized after diagnosis. **(A)** Histological section stain from breast carcinoma (HE  $\times 200$ ); **(B)** CD3 IHC stain in breast carcinoma highlighted numerous CD3+ T cells in the infiltrating front of neoplasia ( $\times 200$ ); **(C)** CD20 IHC stain showed a similar distribution of CD20+ B cells compared with CD3+ T lymphocytes ( $\times 200$ ); **(D)** CD4 IHC stain revealed that most lymphocytes are CD4+ T cells ( $\times 200$ ); **(E)** CD8 IHC stain highlighted less CD8+ T cells but nearest to the tumor in the infiltrating front ( $\times 200$ ).

some tumor-infiltrating T cells, confirming a possible role of B cells as APC in the tumor microenvironment.

*In vitro* stimulation was performed by co-culturing TNBC-T cell with irradiated XABCL-LCL and comparing with control

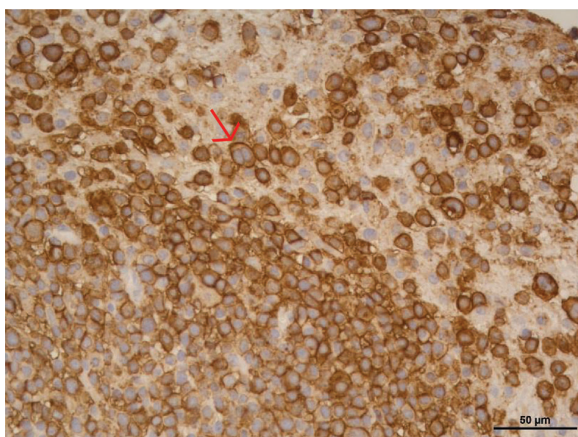


**FIGURE 2** | The tumor derived from a TNBC patient implanted in a PDX was a B-cell lymphocytic tumor (XABCL). CD20 immunohistochemical stain in the histological section revealed that most of the cells were CD20+ B cells. Cells with a bilobed nucleus, reminding of the Reed-Sternberg cells associated with Hodgkin's lymphoma, were observed (pointed with a red arrow).

TNBC-T cells expanded in the presence of OKT3 (anti-human CD3). The TCR repertoire and T-cell phenotypic changes after co-culture were analyzed by TCR HTS and flow cytometry, respectively. A low number of sequences (73 clonotypes) with very low TCR diversity were obtained after co-culture (**Figure 4A** and **Supplementary Table 3**), also displaying a pattern different from the OKT3 control (**Figure 4B** and **Supplementary Figure 3A**).

Only two of the five shared sequences between XABCL tissue and TNBC-T cells (**Figure 3A**) were maintained, i.e., CARSTNGELFF (TRBV28) and CSARVPGLPDTQYF (TRBV20-1) (**Supplementary Figure 3B**). These two clonotypes were also found in the control T-cell cultures expanded with anti-CD3, but the CARSTNGELFF sequence represented a larger normalized fraction after the co-culture with the XABCL-LCL. Phenotypic analysis (**Supplementary Figure 3C**) showed little differences other than a decrease of the double-negative (DN) T-cell population, which represented 41.8% of T cells in the initial culture and only 1.34% after co-culture. This subset appeared to be replaced by CD4+ T cells, varying from 15% in the initial culture to 43.6% after co-culture. CD8+ T cells displayed similar frequencies in both samples: 40.6% and 52.1% in the initial culture and after co-culture, respectively. Thus, the results of the *in vitro* experiments confirmed that, even after transformed to an LCL, B cells derived from the XABCL tumor influenced the TCR repertoire of the infiltrating T cells.





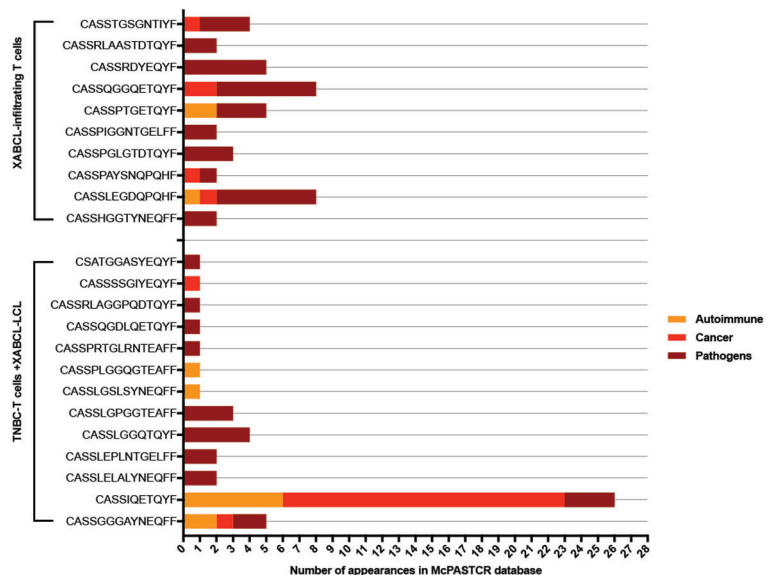


**FIGURE 5** | TCR sequences from XABCL-infiltrating T cells and TNBC-T cells expanded in the presence of XABCL-LCL found in the McPAS-TCR database. Ten sequences from the 43 clonotypes (23%) infiltrating the XABCL tissue had been previously reported as TCR sequences recognizing pathogens. From these, 50% had also been described in non-communicable diseases, i.e., cancer and autoimmunity. One sequence had been identified in the three pathologies. From the T cells expanded *in vitro* in the presence of XABCL-LCL, 13 clonotypes were found in the literature: 8, 2, and 1 of these had been exclusively identified in pathogen infections, autoimmunity, and cancer, respectively, and 2 sequences had been described in the three categories, but remarkably the CASSIQETQYF sequence had been identified several times in cancer.

viruses itself has also been proposed to be related with autoimmune and inflammatory processes in several cases (24, 25, 63). Thus, the presence of EBV+ B cells, as well as other virus-infected cells, in an immunomodulated microenvironment together with ICPI treatment may be an additional factor with a role in the development of irAEs.

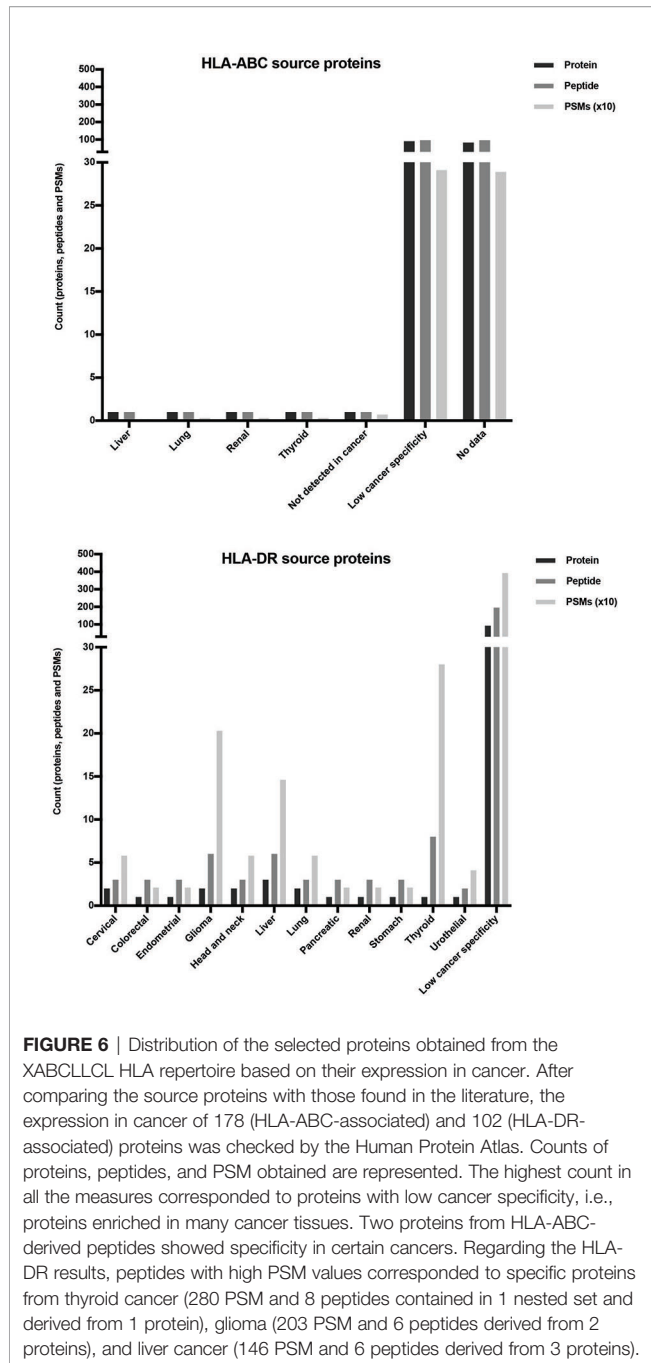
In the last years, different groups have performed analysis of the association between infection by different species of human herpesvirus (HHV) such as EBV (or HHV-4) (64) and cytomegalovirus (CMV or HHV-5) (65), or retrovirus such as human T-lymphotropic virus (HTLV) (66), and the tumor outcomes. However, these studies are all focused on the direct role of the viruses in the development of tumors but not in the contribution of the antivirus responses to the antitumor response. In this research, we have been able to study different immune-related factors associated with the presence of EBV+ B cells among TIL. We have studied a TNBC biopsy obtained before neoadjuvant chemotherapy and a XABCL lymphocytic tumor generated from a simultaneously obtained biopsy, as well as T cells derived from the TNBC (TNBC-T cells) and the EBV+ B cell line derived from the XABCL (XABCL-LCL).

IHC of the biopsy of the patient first revealed that most of the CD3+ T cells found in the histological section were CD4+ T cells colocalized with CD20+ cells, while CD8+ T cells were localized nearest to the tumor in the infiltrating front of neoplasia. This would suggest a possible *in situ* interaction between B cells and Th. Since B cells can act as professional APC, the presence of B cells, even if they are not tumor-specific, can contribute to tune

the tumor landscape. The role of B cells as a putative inducer of the T-cell response in the tumoral microenvironment in BC is still unclear (67).

The XABCL generated from the TNBC biopsy resulted in a lymphocytic tumor; XABCL-LCL was CD19+, CD20+, CD21-, and CD38+, an activated germinal center B-cell phenotype. We confirmed that the XABCL-LCL, as well as the PBMCs of the patient, was EBV+. This is not surprising since up to 40% of Hodgkin's lymphomas are EBV-associated and LCLs can be generated *in vitro* using EBV. Considering that EBV is detected in more than 90% of the adult population of the world (68) and that it has the ability to be maintained for life in a latent stage, it is not unexpected that among TIL there were EBV+ B cells. The development of EBV+ lymphocytic neoplasms in PDX derived from breast cancer had also been previously described (10). This can be explained by the lack of a mature immune system in the PDX models, which are NSG mice, and the evidence that EBV infection more frequently leads to lymphoproliferative disorders in immunosuppressive contexts (20, 69, 70). We are not aware that these XABCLs have been used before as a model to investigate the role of tumor-infiltrating EBV+ B cells.

The BCR analysis of the XABCL revealed a unique BCR sequence representing the major fraction in both the tissue and the LCL. This confirmed that the conversion into a lymphocytic tumor was produced in the mice and not by the establishment of an LCL *in vitro*. We analyzed the BCR repertoire in the initial patient biopsy, and this BCR sequence was found in the TNBC, among many other BCR sequences.



Interestingly, the histological section obtained from the first pass of the XABCL tumor revealed some CD3+ T cells infiltrating the tumor. TCR sequencing confirmed that some T cells were still maintained after the third XABCL pass. Forty-three clonotypes were obtained and 18 of these were also found in the TNBC frozen tissue or in the expanded TNBC-T cells. The maintenance of T cells in the XABCL during the three passes in mice may be the result of stimulation by the XABCL B cells, which expressed the HLA class I and class II molecules as well as the costimulatory molecules CD80, CD86, and PD-L1. An

increased expression of the HLA molecules is usually observed in EBV+ B cells (63). Moreover, a different pattern of TCR was observed in the TNBC samples compared with the XABCL B cells. Therefore, we used TNBC-T cells for co-culture with irradiated XABCL-LCL to study if a T-cell selection could also be observed *in vitro*. Upon interaction with the XABCL-LCL, 73 clonotypes were identified and a decrease in TCR diversity was observed. Two of the sequences expanded were previously found in the XABCL, i.e., CARSTNGELFF (TRBV28) and CSARVPLPDTQYF (TRBV20-1). Certain clonotypes found in the initial cultures were maintained in the XABCL-LCL-expanded TNBC-T cells, but not in the control. Thus, these results altogether suggest that some EBV+ B cells may be able to stimulate T cells from TIL, inducing a certain selection of the TCR repertoire.

The peptide repertoire presented by HLA-ABC and HLA-DR in the XABCL-LCL was analyzed. We did not find EBV-derived peptides neither in the class I nor in the class II analysis. This is not very surprising since EBNA1 is the only viral protein expressed in all EBV-associated malignant diseases (71). The subcellular location of source proteins showed a pattern common to B-cell line repertoires (53, 54). The clustering analysis obtained revealed two binding motifs matching the HLA haplotype of the patient. It is worth mentioning that in the HLA-DR study, the most abundant source protein was GAPDH, and although it is a commonly found protein, it is not that frequent to find HLA-DR-associated GAPDH peptides in high abundance. A relationship between GAPDH with breast cancer has been described (72, 73); therefore, it could be interesting to further analyze the relevance of the GAPDH-derived peptides presented by these cells.

There are several studies of the HLA class I and class II repertoire using LCL, but these are transformed *in vitro* while the XABCL B cells used in this study were infected and transformed by the EBV *in vivo*. Therefore, there could be differences in the peptide repertoire between these cells and the typical LCL. In order to study this, we excluded the source proteins from the peptides obtained from LCL found in the literature, independently for the class I (39–44) and the class II alleles (45–54). The resulting protein pool represented 16% and 23% of the total source proteins obtained from the HLA-ABC and the HLA-DR peptidomes, respectively. These proteins were mostly involved in the antigen processing and presentation and in the phagosome pathways. This indicates that these cells may present some different proteins compared with other LCL and that these B cells still can act as APC.

Many of the selected sequences were derived from proteins that can be present in many cancer tissues, catalogued as proteins with low cancer specificity. Nevertheless, some proteins enriched in cancer were also found, especially in the HLA-DR selected peptides. Thus, in a tumoral microenvironment, peptides derived from autologous proteins as cancer-enriched proteins can be presented by these B cells. In the future, these peptides should be used separately *in vitro* to analyze their capacity to stimulate cancer-infiltrating T cells.

Several features of EBV+ B cells make them relevant in the tumor context. Because tumor cells are known to downregulate the HLA molecules to escape from immune response, the activation and maintenance of both CD4+ and CD8+ T cells in the tumor site is usually the responsibility of APC. The role of B cells as modulators of the antitumoral response has been latterly considered (74). However, EBV+ B cells in a latent stage are memory-like B cells activated by signaling pathways similar with those produced by the CD40L-mediated activation (75), in the absence of T-cell signals and regardless of their BCR specificity. Moreover, EBV+ B cells in a latent stage have an abnormal transcriptome (76). On the other hand, although EBV-specific T cells are maintained throughout life, participating in a persistent control of the infection, the immunomodulatory capacities of the tumor cells affecting the microenvironment may give the EBV a chance to start an infectious stage and to escape the immune response. Two recent studies have reported fatal inflammations [encephalitis (25) and myocarditis (24)] in post-ICPI melanoma patients, in which EBV-specific T cells were involved. Even so, the antigens responsible for these dysregulations may not be limited to EBV-derived antigens.

In summary, this is a first proof of concept that gives relevance to EBV+ B cells present in the tumor site. We have not only demonstrated their presence but also that they are in an activated status and able to stimulate T cells from TIL. Our data also evidence that EBV+ B cells can modulate the TCR repertoire as a certain pattern has been identified and some of the TCR sequences maintained had been already reported in the literature. Certain uncommon peptides presented by HLA-ABC and HLA-DR molecules have been also identified. Thus, to take profit of the XABCL tumors can be a tool to understand the role of EBV+ B cells in the tumor infiltrates and how they can contribute to different patient outcomes by shaping the TCR repertoire.

## DATA AVAILABILITY STATEMENT

The datasets presented in this study can be found in online repositories. TCR sequencing data from the TNBC-derived T cell cultures are available as SRA accessions in the BioProject PRJNA75917. The TCR and BCR HTS from TNBC and XABCL biopsies are available as an ImmuneAccess Project (DOI <https://doi.org/10.21417/AA2021FI>). The mass spectrometry proteomics data have been deposited to the

ProteomeXchange Consortium via the PRIDE (77) partner repository with the dataset identifier PXD028646.

## AUTHOR CONTRIBUTIONS

Conceptualization: AA and MM. Methodology: AA, MM, CR-M, MC, EM, and YA. Investigation: AA, VP, RR, EM, and YA. Resources: VP, RR, CB, EZ, JA, and MC. Writing—original draft: AA and MM. Writing—review and editing: AA, MC, JC, and MM. Supervision: JC and MM. All authors contributed to the article and approved the submitted version.

## FUNDING

This project was funded by Roche Farma, S.A. grant SP181123001 and the Spanish Ministry of Science, Innovation and Universities grant RTI2018-097414-B-I00. Partial financial support was received from the “El Paseico de la Mama” 2015. This study received partial funding from Roche Farma, S.A. The funders were not involved in the study design, collection, analysis, interpretation of data, the writing of this article, or the decision to submit it for publication.

## ACKNOWLEDGMENTS

We want to particularly thank the patient for participating in this study. We thank the SCAC and the SGB services of the IBB-MRB (UAB, Bellaterra), especially Manuela Costa, for the help in the experimental procedures. We acknowledge A. González, Ph.D., and M. Juan, M.D., Ph.D., from Hospital Clinic Barcelona (Barcelona) for the support in the BCR sequencing. We also want to acknowledge Prof. D. Jaraquemada from the Immunology Unit (Cellular Biology, Physiology and Immunology Department, UAB, Bellaterra) for the help in the peptide analysis and for the thorough revision of the manuscript.

## SUPPLEMENTARY MATERIAL

The Supplementary Material for this article can be found online at: <https://www.frontiersin.org/articles/10.3389/fimmu.2021.761798/full#supplementary-material>

## REFERENCES

- Gao G, Wang Z, Qu X, Zhang Z. Prognostic Value of Tumor-Infiltrating Lymphocytes in Patients With Triple-Negative Breast Cancer: A Systematic Review and Meta-Analysis. *BMC Cancer* (2020) 20:179. doi: 10.1186/s12885-020-6668-z
- Quintana Á, Peg V, Prat A, Moliné T, Villacampa G, Paré L, et al. Immune Analysis of Lymph Nodes in Relation to the Presence or Absence of Tumor Infiltrating Lymphocytes in Triple-Negative Breast Cancer. *Eur J Cancer* (2021) 148:134–45. doi: 10.1016/j.ejca.2021.01.037
- Kuroda H, Jamiyan T, Yamaguchi R, Kakumoto A, Abe A, Harada O, et al. Tumor-Infiltrating B Cells and T Cells Correlate With Postoperative Prognosis in Triple-Negative Carcinoma of the Breast. *BMC Cancer* (2021) 21:286. doi: 10.1186/s12885-021-08009-x
- Shimabukuro-Vornhagen A, Schlößer HA, Gryschock L, Malcher J, Wennhold K, Garcia-Marquez M, et al. Characterization of Tumor-Associated B-Cell Subsets in Patients With Colorectal Cancer. *Oncotarget* (2014) 5:4651–64. doi: 10.18632/oncotarget.1701
- Nielsen JS, Sahota RA, Milne K, Kost SE, Nesslinger NJ, Watson PH, et al. CD20+ Tumor-Infiltrating Lymphocytes Have an Atypical CD27- Memory

- Phenotype and Together With CD8+ T Cells Promote Favorable Prognosis in Ovarian Cancer. *Clin Cancer Res* (2012) 18:3281–92. doi: 10.1158/1078-0432.CCR-12-0234
6. Garnelo M, Tan A, Her Z, Yeong J, Lim CJ, Chen J, et al. Interaction Between Tumour-Infiltrating B Cells and T Cells Controls the Progression of Hepatocellular Carcinoma. *Gut* (2017) 66:342–51. doi: 10.1136/gutjnl-2015-310814
  7. Petitprez F, De Reyniès A, Keung EZ, Chen TW-W, Sun C-M, Calderaro J, et al. B Cells are Associated With Survival and Immunotherapy Response in Sarcoma. *Nature* (2020) 577:556–60. doi: 10.1038/s41586-019-1906-8
  8. Bruno TC, Ebner PJ, Moore BL, Squalls OG, Waugh KA, Eruslanov EB, et al. Antigen-Presenting Intratumoral B Cells Affect CD4+ TIL Phenotypes in Non-Small Cell Lung Cancer Patients. *Cancer Immunol Res* (2017) 5:898–907. doi: 10.1158/2326-6066.CIR-17-0075
  9. Epstein MA, Achong BG, Barr YM. Virus Particles in Cultured Lymphoblasts From Burkitt's Lymphoma. *Lancet* (1964) 1:702–3. doi: 10.1016/S0140-6736(64)91524-7
  10. Bondarenko G, Ugolkov A, Rohan S, Kulesza P, Dubrovskiy O, Gursel D, et al. Patient-Derived Tumor Xenografts Are Susceptible to Formation of Human Lymphocytic Tumors. *Neoplasia* (2015) 17:735–41. doi: 10.1016/j.neo.2015.09.004
  11. Pannone G, Zamparese R, Pace M, Pedicillo MC, Cagiano S, Somma P, et al. The Role of EBV in the Pathogenesis of Burkitt's Lymphoma: An Italian Hospital Based Survey. *Infect Agents Cancer* (2014) 9:34. doi: 10.1186/1750-9378-9-34
  12. Küppers R. The Biology of Hodgkin's Lymphoma. *Nat Rev Cancer* (2009) 9:15–27. doi: 10.1038/nrc2542
  13. Massini G, Siemer D, Hohaus S. EBV in Hodgkin Lymphoma. *Mediterr J Hematol Infect Dis* (2009) 1:e2009013. doi: 10.4084/MJHID.2009.013
  14. Carbone A, Ghoghini A, Dotti G. EBV-Associated Lymphoproliferative Disorders: Classification and Treatment. *Oncologist* (2008) 13:577–85. doi: 10.1634/theoncologist.2008-0036
  15. Green M, Michaels MG. Epstein–Barr Virus Infection and Posttransplant Lymphoproliferative Disorder. *Am J Transplant* (2013) 13:41–54. doi: 10.1111/ajt.12004
  16. Stern J, Miller G, Li X, Saxena D. Virome and Bacteriome: Two Sides of the Same Coin. *Curr Opin Virol* (2019) 37:37–43. doi: 10.1016/j.coviro.2019.05.007
  17. Shannon-Lowe C, Rickinson A. The Global Landscape of EBV-Associated Tumors. *Front Oncol* (2019) 9:713. doi: 10.3389/fonc.2019.00713
  18. Hicklin DJ, Marincola FM, Ferrone S. HLA Class I Antigen Downregulation in Human Cancers: T-Cell Immunotherapy Revives an Old Story. *Mol Med Today* (1999) 5:178–86. doi: 10.1016/S1357-4310(99)01451-3
  19. Tangye SG, Latour S. Primary Immunodeficiencies Reveal the Molecular Requirements for Effective Host Defense Against EBV Infection. *Blood* (2020) 135:644–55. doi: 10.1182/blood.2019000928
  20. Shannon-Lowe C, Rickinson AB, Bell AI. Epstein–Barr Virus-Associated Lymphomas. *Philos Trans R Soc Lond B Biol Sci* (2017) 372:20160271. doi: 10.1098/rstb.2016.0271
  21. John T, Yanagawa N, Kohler D, Craddock KJ, Bandarchi-Chamkhaleh B, Pintilie M, et al. Characterization of Lymphomas Developing in Immunodeficient Mice Implanted With Primary Human non-Small Cell Lung Cancer. *J Thorac Oncol* (2012) 7:1101–8. doi: 10.1097/JTO.0b013e3182519d4d
  22. Dieter SM, Giessler KM, Kriegsmann M, Dubash TD, Möhrmann L, Schulz ER, et al. Patient-Derived Xenografts of Gastrointestinal Cancers are Susceptible to Rapid and Delayed B-Lymphoproliferation. *Int J Cancer* (2017) 140:1356–63. doi: 10.1002/ijc.30561
  23. Long HM, Meckiff BJ, Taylor GS. The T-Cell Response to Epstein-Barr Virus–New Tricks From an Old Dog. *Front Immunol* (2019) 10:2193. doi: 10.3389/fimmu.2019.02193
  24. Johnson DB, Balko JM, Compton ML, Chalkias S, Gorham J, Xu Y, et al. Fulminant Myocarditis With Combination Immune Checkpoint Blockade. *N Engl J Med* (2016) 375:1749–55. doi: 10.1056/NEJMoa1609214
  25. Johnson DB, McDonnell WJ, Gonzalez-Ericsson PI, Al-Rohil RN, Mobley BC, Salem J-E, et al. A Case Report of Clonal EBV-Like Memory CD4+ T Cell Activation in Fatal Checkpoint Inhibitor-Induced Encephalitis. *Nat Med* (2019) 25:1243–50. doi: 10.1038/s41591-019-0523-2
  26. Riddell SR, Greenberg PD. The Use of Anti-CD3 and Anti-CD28 Monoclonal Antibodies to Clone and Expand Human Antigen-Specific T Cells. *J Immunol Methods* (1990) 128:189–201. doi: 10.1016/0022-1759(90)90210-M
  27. Bolotin DA, Poslavsky S, Mitrophanov I, Shugay M, Mamedov IZ, Putintseva EV, et al. MiXCR: Software for Comprehensive Adaptive Immunity Profiling. *Nat Methods* (2015) 12:380–1. doi: 10.1038/nmeth.3364
  28. Shugay M, Bagaev DV, Turchaninova MA, Bolotin DA, Britanova OV, Putintseva EV, et al. VDJtools: Unifying Post-Analysis of T Cell Receptor Repertoires. *PLoS Comput Biol* (2015) 11:e1004503. doi: 10.1371/journal.pcbi.1004503
  29. Tickotsky N, Sagiv T, Prilusky J, Shifrut E, Friedman N. McPAS-TCR: A Manually Curated Catalogue of Pathology-Associated T Cell Receptor Sequences. *Bioinformatics* (2017) 33:2924–9. doi: 10.1093/bioinformatics/btx286
  30. R Core Team. R: A Language and Environment for Statistical Computing. In: *R Foundation for Statistical Computing*. Vienna, Austria (2019) Available at: <https://www.R-project.org/>.
  31. Wickham H, François R, Henry L, Müller KRStudio. *Dplyr: A Grammar of Data Manipulation*. (2020). Available at: <https://CRAN.R-project.org/package=dplyr>.
  32. Neuwirth E. *RColorBrewer: ColorBrewer Palettes*. (2014). Available at: <https://CRAN.R-project.org/package=RColorBrewer>.
  33. Conway JR, Lex A, Gehlenborg N. UpSetR: An R Package for the Visualization of Intersecting Sets and Their Properties. *Bioinformatics* (2017) 33:2938–40. doi: 10.1093/bioinformatics/btx364
  34. Heyder T, Kohler M, Tarasova NK, Haag S, Rutishauser D, Rivera NV, et al. Approach for Identifying Human Leukocyte Antigen (HLA)-DR Bound Peptides From Scarce Clinical Samples. *Mol Cell Proteomics* (2016) 15:3017–29. doi: 10.1074/mcp.M116.060764
  35. Stepniak D, Wiesner M, de Ru AH, Moustakas AK, Drijfhout JW, Papadopoulos GK, et al. Large-Scale Characterization of Natural Ligands Explains the Unique Gluten-Binding Properties of HLA-Dq2. *J Immunol* (2008) 180:3268–78. doi: 10.4049/jimmunol.180.5.3268
  36. Consortium TU. UniProt: A Worldwide Hub of Protein Knowledge. *Nucleic Acids Res* (2019) 47:D506–15. doi: 10.1093/nar/gky1049
  37. Huang DW, Sherman BT, Lempicki RA. Systematic and Integrative Analysis of Large Gene Lists Using DAVID Bioinformatics Resources. *Nat Protoc* (2009) 4:44–57. doi: 10.1038/nprot.2008.211
  38. Huang DW, Sherman BT, Lempicki RA. Bioinformatics Enrichment Tools: Paths Toward the Comprehensive Functional Analysis of Large Gene Lists. *Nucleic Acids Res* (2009) 37:1–13. doi: 10.1093/nar/gkn923
  39. Caron E, Espona L, Kowalewski DJ, Schuster H, Ternette N, Alpizar A, et al. An Open-Source Computational and Data Resource to Analyze Digital Maps of Immunopeptidomes. *eLife* (2015) 4:e07661. doi: 10.7554/eLife.07661
  40. Bassani-Sternberg M, Pletscher-Frankild S, Jensen LJ, Mann M. Mass Spectrometry of Human Leukocyte Antigen Class I Peptidomes Reveals Strong Effects of Protein Abundance and Turnover on Antigen Presentation. *Mol Cell Proteomics* (2015) 14:658–73. doi: 10.1074/mcp.M114.042812
  41. Granados DP, Yahyaoui W, Laumont CM, Daouda T, Muratore-Schroeder TL, Côté C, et al. MHC I-associated Peptides Preferentially Derive From Transcripts Bearing miRNA Response Elements. *Blood* (2012) 119:e181–91. doi: 10.1182/blood-2012-02-412593
  42. Lanoix J, Durette C, Courcelles M, Cossette É, Comtois-Marotte S, Hardy M-P, et al. Comparison of the MHC I Immunopeptidome Repertoire of B-Cell Lymphoblasts Using Two Isolation Methods. *Proteomics* (2018) 18:e1700251. doi: 10.1002/pmic.201700251
  43. Liepe J, Marino F, Sidney J, Jeko A, Bunting DE, Sette A, et al. A Large Fraction of HLA Class I Ligands are Proteasome-Generated Spliced Peptides. *Science* (2016) 354:354–8. doi: 10.1126/science.aaf4384
  44. Schellens IMM, Hoof I, Meiring HD, Spijkers SNM, Poelen MCM, Brink JAM, et al. Comprehensive Analysis of the Naturally Processed Peptide Repertoire: Differences Between HLA-A and B in the Immunopeptidome. *PLoS One* (2015) 10:e0136417. doi: 10.1371/journal.pone.0136417
  45. Lippolis JD, White FM, Marto JA, Luckey CJ, Bullock TNJ, Shabanowitz J, et al. Analysis of MHC Class II Antigen Processing by Quantitation of Peptides That Constitute Nested Sets. *J Immunol* (2002) 169:5089–97. doi: 10.4049/jimmunol.169.9.5089

46. Dengjel J, Schoor O, Fischer R, Reich M, Kraus M, Muller M, et al. Autophagy Promotes MHC Class II Presentation of Peptides From Intracellular Source Proteins. *Proc Natl Acad Sci* (2005) 102:7922–7. doi: 10.1073/pnas.0501190102
47. Verreck FAW, van de Poel A, Drijfhout JW, Amons R, Coligan JE, Koning F. Natural Peptides Isolated From Glyc6/Va186-Containing Variants of HLA-DR1, -DR11, -DR13, and -DR52. *Immunogenetics* (1996) 43:392–7. doi: 10.1007/BF02199809
48. Futaki G, Kobayashi H, Sato K, Taneichi M, Katagiri M. Naturally Processed HLA-DR9/DR53 (DRB1\*0901/DRB4\*0101)-Bound Peptides. *Immunogenetics* (1995) 42:299–301. doi: 10.1007/BF00176449
49. Davenport MP, Quinn CL, Chicz RM, Green BN, Willis AC, Lane WS, et al. Naturally Processed Peptides From Two Disease-Resistance-Associated HLA-DR13 Alleles Show Related Sequence Motifs and the Effects of the Dimorphism at Position 86 of the HLA-DR13 Chain. *Proc Natl Acad Sci USA* (1995) 92:6567–71. doi: 10.1073/pnas.92.14.6567
50. Falk K, Rötzschke O, Stevanovic S, Jung G, Rammensee H-G. Pool Sequencing of Natural HLA-DR, DQ, and DP Ligands Reveals Detailed Peptide Motifs, Constraints of Processing, and General Rules. *Immunogenetics* (1994) 39:230–42. doi: 10.1007/BF00188785
51. Chicz RM, Urban RG, Lane WS, Gorga JC, Stern LJ, Vignali DA, et al. Predominant Naturally Processed Peptides Bound to HLA-DR1 are Derived From MHC-Related Molecules and are Heterogeneous in Size. *Nature* (1992) 358:764–8. doi: 10.1038/358764a0
52. Chicz RM, Urban RG, Gorga JC, Vignali DA, Lane WS, Strominger JL. Specificity and Promiscuity Among Naturally Processed Peptides Bound to HLA-DR Alleles. *J Exp Med* (1993) 178:27–47. doi: 10.1084/jem.178.1.27
53. Muixí L, Gay M, Muñoz-Torres PM, Guitart C, Cedano J, Abian J, et al. The Peptide-Binding Motif of HLA-DR8 Shares Important Structural Features With Other Type 1 Diabetes-Associated Alleles. *Genes Immun* (2011) 12:504–12. doi: 10.1038/gene.2011.26
54. Alvarez I, Collado J, Daura X, Colomé N, Rodríguez-García M, Gallart T, et al. The Rheumatoid Arthritis-Associated Allele HLA-DR10 (DRB1\*1001) Shares Part of its Repertoire With HLA-DR1 (DRB1\*0101) and HLA-DR4 (DRB\*0401). *Arthritis Rheum* (2008) 58:1630–9. doi: 10.1002/art.23503
55. Andreatta M, Alvarez B, Nielsen M. GibbsCluster: Unsupervised Clustering and Alignment of Peptide Sequences. *Nucleic Acids Res* (2017) 45:W458–63. doi: 10.1093/nar/gkx248
56. Reynisson B, Barra C, Kaabinejadian S, Hildebrand WH, Peters B, Nielsen M. Improved Prediction of MHC II Antigen Presentation Through Integration and Motif Deconvolution of Mass Spectrometry MHC Eluted Ligand Data. *J Proteome Res* (2020) 19:2304–15. doi: 10.1021/acs.jproteome.9b00874
57. *The Human Protein Atlas*. Available at: <https://www.proteinatlas.org/>.
58. Pontén F, Jirstrom K, Uhlen M. The Human Protein Atlas - a Tool for Pathology. *J Pathol* (2008) 216:387–93. doi: 10.1002/path.2440
59. Uhlen M, Zhang C, Lee S, Sjostedt E, Fagerberg L, Bidkhori G, et al. A Pathology Atlas of the Human Cancer Transcriptome. *Science* (2017) 357: ean2507. doi: 10.1126/science.aan2507
60. Wu AA, Drake V, Huang H-S, Chiu S, Zheng L. Reprogramming the Tumor Microenvironment: Tumor-Induced Immunosuppressive Factors Paralyze T Cells. *Oncoimmunology* (2015) 4:e1016700. doi: 10.1080/2162402X.2015.1016700
61. Seidel JA, Otsuka A, Kabashima K. Anti-PD-1 and Anti-CTLA-4 Therapies in Cancer: Mechanisms of Action, Efficacy, and Limitations. *Front Oncol* (2018) 8:86. doi: 10.3389/fonc.2018.00086
62. Liu Y-H, Zang X-Y, Wang J-C, Huang S-S, Xu J, Zhang P. Diagnosis and Management of Immune Related Adverse Events (irAEs) in Cancer Immunotherapy. *Biomed Pharmacotherapy* (2019) 120:109437. doi: 10.1016/j.biopha.2019.109437
63. Morandi E, Jagessar SA, Hart BA, Gran B. EBV Infection Empowers Human B Cells for Autoimmunity: Role of Autophagy and Relevance to Multiple Sclerosis. *J Immunol* (2017) 199:435–48. doi: 10.4049/jimmunol.1700178
64. Abdallah MOE, Algizouli UK, Suliman MA, Abdulrahman RA, Koko M, Fessahaye G, et al. EBV Associated Breast Cancer Whole Methyloome Analysis Reveals Viral and Developmental Enriched Pathways. *Front Oncol* (2018) 8:316. doi: 10.3389/fonc.2018.00316
65. Paradowska E, Jabłońska A, Studzińska M, Wilczyński M, Wilczyński JR. Detection and Genotyping of CMV and HPV in Tumors and Fallopian Tubes From Epithelial Ovarian Cancer Patients. *Sci Rep* (2019) 9:1–10. doi: 10.1038/s41598-019-56448-1
66. Du G, Zhang W, Zhang Z, Zeng M, Wang Y. HTLV-1-Associated Genes as Potential Biomarkers for Endometrial Cancer. *Oncol Lett* (2019) 18:699–705. doi: 10.3892/ol.2019.10389
67. Garaud S, Buisseret L, Solinas C, Gu-Trantien C, de Wind A, den Eynden GV, et al. Tumor-Infiltrating B Cells Signal Functional Humoral Immune Responses in Breast Cancer. *JCI Insight* (2019) 4:e219641. doi: 10.1172/jci.insight.129641
68. Smatti MK, Al-Sadeq DW, Ali NH, Pintus G, Abou-Saleh H, Nasrallah GK. Epstein-Barr Virus Epidemiology, Serology, and Genetic Variability of LMP-1 Oncogene Among Healthy Population: An Update. *Front Oncol* (2018) 8:211. doi: 10.3389/fonc.2018.00211
69. Strowig T, Gurur C, Ploss A, Liu Y-F, Arrey F, Sashihara J, et al. Priming of Protective T Cell Responses Against Virus-Induced Tumors in Mice With Human Immune System Components. *J Exp Med* (2009) 206:1423–34. doi: 10.1084/jem.20081720
70. Fujiwara S, Nakamura H. Animal Models for Gammaherpesvirus Infections: Recent Development in the Analysis of Virus-Induced Pathogenesis. *Pathogens* (2020) 9:116. doi: 10.3390/pathogens9020116
71. Krüger S, Schroers R, Rooney CM, Gahn B, Chen S-Y. Identification of a Naturally Processed HLA-DR-Restricted T-Helper Epitope in Epstein-Barr Virus Nuclear Antigen Type 1. *J Immunother* (2003) 26:212–21. doi: 10.1097/00002371-200305000-00005
72. Valenti MT, Bertoldo F, Dalle Carbonare L, Azzarello G, Zenari S, Zanatta M, et al. The Effect of Bisphosphonates on Gene Expression: GAPDH as a Housekeeping or a New Target Gene? *BMC Cancer* (2006) 6:49. doi: 10.1186/1471-2407-6-49
73. Révillon F, Pawlowski V, Hornez L, Peyrat JP. Glyceraldehyde-3-Phosphate Dehydrogenase Gene Expression in Human Breast Cancer. *Eur J Cancer* (2000) 36:1038–42. doi: 10.1016/S0959-8049(00)00051-4
74. Sharonov GV, Serebrovskaya EO, Yuzhakova DV, Britanova OV, Chudakov DM. B Cells, Plasma Cells and Antibody Repertoires in the Tumour Microenvironment. *Nat Rev Immunol* (2020) 20:294–307. doi: 10.1038/s41577-019-0257-x
75. Neparidze N, Lacy J. Malignancies Associated With Epstein-Barr Virus: Pathobiology, Clinical Features, and Evolving Treatments. *Clin Adv Hematol Oncol* (2014) 12:358–71.
76. Mrozek-Gorska P, Buschle A, Pich D, Schwarzmayr T, Fechtner R, Scialdone A, et al. Epstein-Barr Virus Reprograms Human B Lymphocytes Immediately in the Prelatent Phase of Infection. *PNAS* (2019) 116:16046–55. doi: 10.1073/pnas.1901314116
77. Perez-Riverol Y, Csordas A, Bai J, Bernal-Llinares M, Hewapathirana S, Kundu DJ, et al. The PRIDE Database and Related Tools and Resources in 2019: Improving Support for Quantification Data. *Nucleic Acids Res* (2019) 47: D442–50. doi: 10.1093/nar/gky1106

**Conflict of Interest:** The authors declare that the research was conducted in the absence of any commercial or financial relationships that could be construed as a potential conflict of interest.

**Publisher's Note:** All claims expressed in this article are solely those of the authors and do not necessarily represent those of their affiliated organizations, or those of the publisher, the editors and the reviewers. Any product that may be evaluated in this article, or claim that may be made by its manufacturer, is not guaranteed or endorsed by the publisher.

Copyright © 2021 Aran, Peg, Rabanal, Bernadó, Zamora, Molina, Arribas, Arribas, Pérez, Roura-Mir, Carrascal, Cortés and Martí. This is an open-access article distributed under the terms of the Creative Commons Attribution License (CC BY). The use, distribution or reproduction in other forums is permitted, provided the original author(s) and the copyright owner(s) are credited and that the original publication in this journal is cited, in accordance with accepted academic practice. No use, distribution or reproduction is permitted which does not comply with these terms.